# $^{1}$H-NMR Based Metabolomics Reveal the Nutrient Differences of Two Kinds of Freshwater Fish Soups Before and After Simulated Gastrointestinal Digestion

Qiongju Cao[a, b, 1], Huili Liu[c,1], Gaonan Zhang [a], Xiaohua Wang [d], Anne Manyande [e], Hongying Du [a, b, *],

[a] Key Laboratory of Environment Correlative Dietology, Ministry of Education, College of Food Science and Technology, Huazhong Agricultural University, Wuhan, Hubei, P.R. China.

[b] National R & D Branch Center for Conventional Freshwater Fish Processing, Wuhan, 430070, Hubei, P.R. China.

[c] Key Laboratory of Magnetic Resonance in Biological Systems, State Key Laboratory of Magnetic Resonance and Atomic and Molecular Physics, Wuhan Institute of Physics and Mathematics, Chinese Academy of Science, P.R. China.

[d] Hubei Provincial Institute for Food Supervision and Test, Wuhan, 430071, P.R. China.

[e] School of Human and Social Sciences, University of West London, London, UK.

[1]: Same contribution to the work

*: Corresponding author

Hongying Du, Email: hydu@mail.hzau.edu.cn, Tel: +86-27-87283007

**Abstract:** Soups show diverse health functions, which could be linked to their original nutrient profiles and metabolites derived from digestion. NMR spectroscopy is a robust and rapid method that unveils or identifies the chemical composition of food or food-derived metabolites. In the current study, $^{1}$H-NMR spectroscopy approach was applied to identify the differences in metabolic profiling of two kinds of home-cooked freshwater fish soups (crucian carp and snakehead fish) before and after *in vitro* gastrointestinal digestion. The nutritional profiles of these soups were studied using the $^{1}$H-NMR method for the first time. Two metabolomics methods -PCA (Principal Component Analysis) and OPLS-DA (Orthogonal Partial Least Squares Discriminant Analysis), were used to analyze the data. On the whole, levels of amino acid metabolites such as valine (Val), tyrosine, choline, taurine (Tau) and glycine were higher in the crucian carp soup, whereas higher levels of fatty acids and unsaturated fatty acids were found in the snakehead soup. Furthermore, the high content of seven metabolites valine, leucine, EPA C20:5 (PUFA eicosapentaenoic acid), acetic acid, taurine, GPCho (phosphatidylcholine) and creatine showed an upward trend after simulated gastrointestinal digestion. The results demonstrate that $^{1}$H-NMR metabolic profile of different fish soups can shed some light to our understanding of food functional properties and dietary therapy. Furthermore, changes of metabolites in digested fish soups could reveal information about chemical compounds which play important roles in the body.

***Keywords:*** *Freshwater fish; Soup; Metabolites; $^{1}$H-NMR; Simulated gastrointestinal digestion;*

## 1. Introduction

Soup is a very popular diet consumed all over the world, and is suitable for people of all ages [1]. Various kinds of fish soups show different dietary therapy functions, which are closely related to their special nutritional components [2]. Freshwater fish is highly regarded and always used in fish soups due to its high level of polyunsaturated fatty acids and is easily digestible. In China, two freshwater fish species (crucian carp and snakehead fish) are frequently prepared into nourishing soup, although their dietary therapy functions are totally different. The snakehead fish soup is usually used as an adjuvant therapy for people with general body weakness and poor nutrition, and also for wound and burns healing[3, 4]. Whereas, the crucian carp soup (CCS) with its attractive milky white color and rich nutrients, has the function of regulating menstruation and lactogenesis, and it is also especially suitable for women who are breastfeeding [5]. These diverse health functions and their associations with different metabolic profiles, should be investigated.

Food metabolic profiling generated by metabolomics [6, 7] is a key approach to understand the nutritional and functional characteristics of food materials or commercial products [8, 9]. Metabolomics is considered to be one of the most powerful approaches for exploring the alterations in metabolite profiles in different samples under different conditions. It has provided vital information for assessing food nutrition, food quality, and food adulteration [10, 11]. Metabolomic analyses have generally been classified as targeted or untargeted approaches. The targeted analyses are known to focus on a specific or small group of intended metabolites that in most cases require accurate quantification [12, 13], and the untargeted or comprehensive metabolomics focus on the detection of as many metabolites as possible in order to obtain the patterns or fingerprints without focusing on specific compounds [14, 15]. The NMR method has been shown to be one of the most robust methodologies through using various technologies for metabolite profiling, especially for a comprehensive analysis of primary food metabolites.

The advantage of $^{1}$H-NMR metabolomics is that it can unambiguously detect a broad range of metabolites without any physical or chemical treatment prior to the statistical analysis[16, 17]. Furthermore, $^{1}$H-NMR spectroscopy combined with pattern recognition and related multivariate statistical methods could offer an efficient way for assessing the metabolic functions [18, 19]. It can also identify significant inherent patterns in a set of indirect measurements that classify objects combined with pattern recognition methods, such as partial least-squares discriminant analysis (PLS-DA) and orthogonal projections to latent structures discriminant analysis (OPLS-DA) [20, 21]. Approaches to PLS-DA or OPLS-DA could reduce the

dimensionality of complex data sets, facilitate the visualization of inherent patterns among the data set and accelerate the interpretation for various functions.

In the current study, metabolomics of two genotypes of freshwater fish soups were explored using an untargeted $^{1}$H-NMR approach. To comprehensively understand the different functions of these two kinds of freshwater fish, the metabolite profiles of different digested states of the fish soups (before and after *in vitro* simulated gastrointestinal digestion) were investigated. Multivariate statistical method OPLS-DA was applied to identify the inherent patterns within $^{1}$H-NMR spectral data, the screened metabolic patterns that potentially ascribe to genotypic diversity and the effect of digestion, plus their interrelationships with various dietary functions. The aim of this work was to establish an effective metabolomics platform for two fish soups, which may partly explain their diversity in dietary therapy.

## 2. Materials and methods

### *2.1. Materials*

Snakehead fish (Channa argus) (~750g, n = 5) and crucian carp (Carassius auratus) (~250g, n = 5) were purchased from the local market in Huazhong Agricultural University, Hubei, China. Each specimen was gutted and cleaned. All the chemicals used were of analytical grade.

### *2.2. Methods*

#### 2.2.1. Preparation of fish soup samples

According to the method described by Tang [22], the handled fish (n=5 for each group) was cooked separately at a suitable raw material/water ratio of 1:4 (*w*/*v*) adopting a stew soup recipe using an induction cooker (RT2134, Midea, China) for 1.5h. Firstly, the power was set at 500W to simmer the soup for 20 min, and then the power was kept at 300W and the soup maintained boiling for 70 min. Before the raw soup samples (without meat and bones) were prepared for $^{1}$H-NMR analysis and further *in vitro* digestion for each group, the filtered soup was divided into four different samples (n=4) for further analysis ($V$ = 10.0 mL for every single test, replication = 4) due to the variation of the homogenization of the soup.

#### 2.2.2. *In vitro* digestion

A two-step process was used to simulate the gastric and intestinal digestion of fish soup using the *in vitro* enzymatic digestion protocol described by Lin et al. [23] with minor modifications. Firstly, the pH of each sample (10.0 mL) was adjusted to 2.0 with 1 M HCl. Pepsin was then added (pepsin/fish soup = 1:25, *w*/*w*), and the mixture incubated at 37 °C for 2 h in a shaking water bath. Next, the pH value was adjusted

to 5.3 with 0.9 M $NaHCO_3$ and further to 7.5 with 1 M NaOH. Then pancreatin was added (pancreatin/fish soup = 1:20, *w*/*w*) and the mixture further incubated at 37 °C for 2.5 h. To terminate the digestion, the test tubes were kept in boiling water for 10 min.

2.2.3. Sample Preparation for $^1$H-NMR Analysis

To avoid the presence of proteins in the solution (both raw and digested soup), the prepared samples and raw fish soup were mixed with 10% (*w*/*w*) trichloroacetic acid (Tca), respectively [24]. To be more specific, each sample of crucian carp and snakehead soup (SS) (*v* = 5.0 mL) was mixed with Tca in equal proportions of 1:1 (*v*/*v*). Then the mixture was centrifuged at 12, 000*g* for 20 min. The supernatants were filtered through 0.45μm filter paper under vacuum. Both raw and digested fish soup samples were stored at -80 °C for $^1$H-NMR detection.

2.2.4. Sample preparation for $^1$H-NMR spectra acquisition

The frozen fish soup solution (raw and digested) was first thawed. Then 300 μL sample was diluted with 240 μL phosphate buffer (*pH*: 7.2; 90 mM $Na_2HPO_4$ and 35 mM $H_2PO_4$) and 60 μL 120mg/L 3-(Trimethylsilyl) propionic - 2, 2, 3, 3, $d_4$ acid sodium salt (TSP, 269913-1G, Sigma-Aldrich) in $D_2O$, and TSP was set as the internal standard and transferred to a 5 mm diameter tube for $^1$H-NMR spectra detection.

2.2.5. $^1$H-NMR Spectra Detection

The measurements of the samples were carried out on a 11.75T BrukerAvance III vertical bore NMR spectrometer (600 MHz for $^1$H) equipped with an inverse cryogenic probe (BrukerBiospin, Germany), and the detectable temperature was kept at 298 K. The NMR detection was completed with a standard WATERGATE pulse sequence [25], which could be used to suppress the water signal. The parameters were set as following: 90° pulse length, 10.5 ms; number of scans, 128; whole data points, 64K; spectral width, 20ppm. The nutritional components in the NMR spectrum were identified based on former publications[26-29], as well as multiplicity, J-coupling values, chemical shifts and 2D NMR spectrum.

The 2D-NMR spectrum included COSY ($^1$H–$^1$H correlation spectroscopy), HSQC ($^1$H–$^{13}$C heteronuclear single quantum correlation) and HMBC ($^1$H–$^{13}$C heteronuclear multiple bond correlation). The 90° pulse length of all 2D-NMR experiments was the same as the $^1$H-NMR spectrum. In COSY experiments, the spectrum (8 transients) was acquired with 2 K data points for each of the 256 increments with a spectral width of 10 ppm for both proton dimensions. HSQC and HMBC NMR spectra were recorded using the gradient selected sequences of 160 transients and 2 K data points for each of the 256

127 increments. The spectral widths were 10 ppm for $^{1}H$ and 220 ppm for $^{13}C$ in HMBC (160 ppm in HSQC)
128 experiments.
129 *2.3. Data analysis*
130 2.3.1. NMR Spectra analysis
131 All the NMR spectral data was analyzed with the commercial software *Topspin* 3.2 (Bruker Biospin,
132 GmbH, Germany) and a home-made software *NMRSpec* in MATLAB (R2014b, Mathworks Inc. 2014) [30,
133 31] (Freely available from the author upon request to jie.wang@wipm.ac.cn [30]).
134 At first, the experimental window function of all the NMR spectra was employed, and the line
135 broadening factor was set to 1 Hz prior to Fourier transformation, then phase and baseline correction were
136 manually corrected in *Topspin*.
137 Chemical shift is the most important parameter for a chemical, and is always affected by various
138 factors, such as instrumental issues, pH value, temperature, salt concentrations, and relative concentrations
139 of specific ions. However, the effect of these factors is not uniform for all the peaks. Thus, it is important
140 to organize the peak alignment before spectral analysis. The region with a strong solvent signal (4.70 -
141 5.2ppm) was excluded prior to further spectral analysis, and the peak alignment was automatically
142 completed in NMRSpec, which is free for researchers and has been successfully utilized to analyze various
143 NMR data [32, 33].
144 In order to show the spectral alignment clearly, the samples from two different kinds of fish after
145 simulated gastrointestinal digestion were illustrated in the current study. To proceed with the peak
146 alignment, all the phase and baseline corrected spectra were initially imported into NMRSpec. After all
147 the $^{1}H$-NMR data were loaded in NMRSpec, and the initial correlation coefficient ($R$) of the spectra was
148 calculated (R=0.9347, Fig. 1A), it was clear to notice that there was slight mismatch in the data. After the
149 spectral alignment in NMRSpec, the $R$ value was increased to 0.9918 and the aligned spectra are illustrated
150 in Fig. 1B. Following the achievement of the spectral alignment, the averaged spectra were calculated in
151 every group (Fig. 2A-2D). Then continuous even spectral bucketing (Size: 0.004 ppm – the common size
152 for spectral analysis [34]) in all spectra was automatically integrated in NMRSpec, and all bucketed spectra
153 data were normalized to the total spectral area before comparing the total concentration differences.
154
155
156

2.3.2. Multivariate Data Analysis

Multivariate data analysis was conducted on the normalized and bucketed NMR data sets in SIMCA (Version 14, Umetrics, Umea, Sweden). The par scaling method was applied to all multivariate analyses. An un-supervised pattern recognition analysis method - Principle component analysis (PCA) was firstly used to reveal the intrinsic variations in the data set and to diagnose any possible outlier if it exists. Then, a supervised orthogonal projection to latent structures discriminate analysis (OPLS-DA) was further applied to screen the major metabolic components which discriminate between the two sample groups. Thus, the metabolic patterns of the special group could be obtained with the help of the OPLS-DA method.

OPLS-DA models were therefore, calculated to find which variables are responsible for discriminating among the following groups: crucian fish soup and snakehead fish soup, crucian fish soup and its digested samples, snakehead fish soup and its digested samples. This simple and robust method has a general applicability for data mining in metabolomics and other similar kinds of data. The quality of the model is defined by the total variance of the components at a confidence level of 95%. R2Y represents the goodness of fit of the representative model, and the overall predictive ability of the model was assessed by cumulative $Q^2$, which represents the fraction of the variation of the Y component that can predict the internal cross-validation of the model. All models were validated applying CV-ANOVA test within SIMCA at $p<0.05$.

The significant varying metabolites were extracted from OPLS-DA correlation coefficient color coded loading plots. The extracted variables were then plotted with standard error in bar graphs using their normalized relative intensities and explained as unique features for the respective fish soups before and after gastrointestinal digestion.

## 3. Results and Discussion

### *3.1 Signal assignment of $^1$H-NMR spectra of raw fish soup and digested fish soup*

The identification of nutritional components in the samples of fish soup was achieved through consulting the research of others[26-29], peak multiplicity, J-coupling, chemical shift and 2D-NMR spectra. As an example, the identified chemicals from a series of 2D-NMR spectra for phenylalanine are shown in Fig. 3 (Including COSY, HSQC and HMBC). All identified chemicals were also verified using several accessible public databases, such as MMCD (URL: http://mmcd.nmrfam.wisc.edu/) and HMDB (URL: http://www.hmdb.ca/). The plausible assignments of the signals in $^1$H-NMR are presented in Fig. 2. They

include: fatty acids; isoleucine; leucine; valine; threonine; lactate; lysine; alanine; eicosapentaenoic fatty acid (ω-3; EPA C20:5); acetic acid; unsaturated fatty acids; linoleic acid (ω-6; C18:2); methionine; docosahexaenoic fatty acid (DHA); glutamate; succinic acid; glutamine; aspartate; asparagine; creatine/creatine phosphate; phenylalanine; choline; phosporylcholine; taurine; glucose; glycine; and ethanol.

When comparing the metabolic profiles of different kinds of fish soups, they were almost in the same state (Fig. 2, groups CCS-2D *vs* SS-2E, and groups DCCS-2A *vs* DSS-2B), although the relative content of every metabolite is not entirely the same (Fig. 2C and 2F). After simulated gastrointestinal digestion, the content of most metabolites in both kinds of samples showed a very clear upward trend (except for lactate and creatine), especially for glucose (Fig. 2, groups CCS-2D *vs* DCCS-2A, and groups SS-2E *vs* DSS-2B). Comparing the metabolic components of these two kinds of fish soups, CCS had higher concentrations of taurine, creatine/ phosphate creatine, glycine, threonine; lactate, and acetic acid, etc., but lower concentrations of phenylalanine and phosporylcholine. After simulated gastrointestinal digestion, DCCS showed higher concentrations of isoleucine, leucine, valine and lysine, etc. However, the concentration of creatine were almost similar. Differences in taurine were uncertain due to the influence of glucose signaling. Although, it is very hard to judge the significant different metabolites among different groups without standard deviation information for comparison, interested readers could roughly estimate the tendency of the metabolites. The variation in the concentration of these metabolites could be linked to the differences of genotypes in fish and simulated *in vitro* digestion. Thus, the difference between the various fish soup samples in the same state was compared (Before and after simulated gastrointestinal digestion).

*3.2 Results of PCA for different kinds of fish soups*

In order to visualize the metabolic discrimination between different kinds of freshwater fish soups before and after *in vitro* gastrointestinal digestion, the un-supervised pattern recognition analysis method – PCA was initially applied to the NMR spectrum to explore the comparative interpretations and the relationships of different kinds of fish soups. PCA is a classic approach requiring no prior knowledge of the data set and acts to reduce the dimensionality of complicated original data whilst generating information within it [35].

In the current study, there were four different kinds of fish soups involved. To discriminate these samples, the nutritional components in $^1$H-NMR spectra were divided into equal widths of 0.004 ppm (2.4 Hz). All the integrated gaps were utilized for PCA. Results of PCA of all the samples are illustrated in Fig. 4, and the first three major components explain 92.7% of all the information inherent in the $^1$H-NMR spectra data set (PC1: 88.3%; PC2: 2.8% and PC3: 1.6%). The quality of the PCA model is described by two statistical parameters $R^2Y$ (cum) and $Q^2$ (cum), and $R^2Y$ represents the goodness of fit and $Q^2$ the predictability of the PCA model [36]. The parameters of $R^2Y$ and $Q^2$ are 97.4% and 95.6%, respectively.

All samples were clearly divided into two different groups, and separated into the 3D major space components. The results show that the metabolites released in the crucian carp soup and snakehead soup are different to some extent (groups *CCS* vs *SS*), which means different genotypes of freshwater fish contain various metabolites in their fish soup. Furthermore, the *in vitro* simulated gastrointestinal digestion had significant effects on these two kinds of soups (*CCS vs DCCS* and *SS vs DSS*). Thus, the characteristics of the metabolites inherent in fish soup changed after the *in vitro* digestive process, as they formed two different clusters as shown in the 3D PC scatter plot. The nutritional components detected with the $^1$H-NMR spectra are representative and could be used to assess the differences of the nutritional profiles of different kinds of fish soup, even after *in vitro* digestion simulation. Finally, all samples in the same state were utilized in the following analysis to screen the most important information.

### *3.3 Statistical analysis*

#### *3.3.1* Comparison of metabolic profiling of different types of freshwater fish soups

The results of PCA for groups SS and CCS are illustrated in Fig. 5A, and the first two major components explain 57.7% of all the information inherent in the $^1$H-NMR spectra data set (PC1: 43.9% and PC2: 13.8%). All samples were separated into two different clusters, and the same group samples were clustered together. Thus it was important to screen the significant different metabolites with other statistical discriminant analysis.

To improve the separation among the different freshwater fish soup samples based on maximizing the covariance between the measured data (X) and the response variable (Y), the loading plot of the OPLS-DA model was utilized to discriminate the two kinds of fish soups. The identity of each group of samples is specified, therefore the maximum variance of the groups could be obtained in the multidimensional space. The OPLS-DA model was applied in order to visualize the metabolic differences as shown in Fig.

5B and Fig. 5C. Complete separation in scores plots of PC1 and PC2 of the OPLS-DA were obtained between the crucian carp soup and snakehead soup before *in vitro* simulated gastrointestinal digestion (Fig. 6A). Moreover, the OPLS-DA model had significantly higher $R^2X$, $R^2Y$, and $Q^2$ values of 0.574, 0.935 and 0.917, respectively, which indicates that it has satisfactory predictive ability. The differences in metabolic profiling among various fish soup samples are important for the identification of key metabolites. The color scale corresponds to the NMR model variable weights (Fig. 5C). The relative changes of metabolites with significant correlation coefficients were a major discriminating factor. Positive and negative peaks indicate relative decrease and increase of metabolite levels in the control groups. Five metabolites, valine, choline, taurine, glycine and an unidentified chemical were much higher in the CCS group.

*3.3.2 Effect of digestion on the nutritional components of fish soups*

The results of the PCA for groups DCCS and DSS are illustrated in Fig. 6A, and the first two major components explain 74.7% of all the information inherent in the $^1$H-NMR spectra data set (PC1: 54.2% and PC2: 20.5%). All samples were almost separated into two different clusters, and the same group samples were clustered together.

To explore the influence of simulated gastrointestinal digestion on the nutritional components of fish soups, the OPLS-DA approach was also applied to distinguish the metabolite differences between CCS and SS after the digestion process. The OPLS-DA model of different states of CCS samples is illustrated in Figs. 6B and 6C, and it was established using one predictive and one orthogonal component in Fig. 6B, and these completely separated into two groups. The parameters of the OPLS-DA model were as following: $R^2X = 0.722$, $R^2Y = 0.836$, $Q^2 = 0.797$, which mean they show good stability and predictability. There are other differences found between these two kinds of samples. It can clearly be seen that the negative signals show higher levels of metabolites in the digested snakehead soup compared to the crucian carp soup, including glucose, taurine, and lactate (Fig. 6C).

*3.4 Metabolic patterns of various fish soup*

Fish soup is one of the most popular diets in China, due to its appetizing taste and source of natural nutritional materials. Various fish species have different functional roles due to their own nutritional profiles. Thus, it is important to compare these two kinds of fish soups - crucian carp and snakehead soups.

From the statistical analysis, several metabolites showed very significant differences in these two different kinds of freshwater fish soups, such as Gly, Tau, Ala and ethanol (Eth) (Fig. 5). Firstly, Eth was only detected in the crucian carp soup probably because it is the most known anoxia-tolerant fish, and easily produces ethanol that serves as the main anaerobic end - product in order to avoid lactic acidosis during prolonged periods of anoxia [37]. But this phenomenon does not occur in the snakehead fish, therefore the Eth was not detected in the snakehead soup. Crucian carp had higher concentrations of Gly and Ala (Fig. 2F and 5C), more than twice the amount in the snakehead soup. Nonetheless umami-taste active amino acids, glycine and alanine have always been regarded as ideal seasoning ingredients [38]. Thus, they are considered as the main contributor to the flavor and appetizing taste of the crucian carp soup [39] .

Taurine is a semi-essential amino acid which is not incorporated into proteins, but has many diverse physiological effects including osmoregulation, bile salt conjugation, membrane stabilization, calcium modulation, anti-oxidation, and immune stimulation [40]. Taurine is prevalent in animal-based foods, especially fish, seafood and meat. Shellfish has very high levels of taurine, and raw shrimp contains almost 180 mg/100 g wet weight. Furthermore, most types of fish are also very good sources of taurine, especially cold-water fish (100-140 mg/100 grams of raw flesh). In the current study, SS had much higher taurine concentration (～2.8 times) than CCS (Fig. 2), which might be related to its function of improving immunity in patients who drink SS after surgery.

Finally, snakehead soup had higher concentration of Ala and Lac (Fig. 2B and 5C). The concentration of Lac is related to anaerobic oxidation of glucose after the animal is dead, and thus can no longer provide any useful nutritional information that is effective. Alanine, also is an intrinsic α–helix stabilizing amino acid which can produce glucose in the liver and plays a crucial role in the glucose-alanine cycle[41] and is beneficial for improving body energy levels.

After the *in vitro* simulated gastrointestinal digestion, most metabolites in these two kinds of soups were increased, especially in glucose levels. The skin and bone of hydrobiont contain mucopolysaccharide [42, 43]. Glycosidic bond cleavage of mucopolysaccharide are known to be linked to dilute hydrochloric acid and produce oligosaccharides and monosaccharides [44]. Mucopolysaccharide could also be hydrolyzed by mucopolysaccharidases such as hyaluronidase and chondroitinase [45]. These may explain the higher content of glucose in the two kinds of soups after *in vitro* simulated gastrointestinal digestion. The differences in nutrient composition between the two kinds of fish may result in differences of metabolic

content between the DSS and the DCCS samples. Comparing these two kinds of soups, DSS samples had higher metabolic content, especially for glucose, taurine, choline and lactate.

## 4. Conclusion

In the present study, the metabolomics approach based on $^{1}$H-NMR spectra was applied to analyze the nutritional characteristics of two kinds of freshwater fish soups before and after *in vitro* simulated digestion. With the help of OPLS-DA methods, different groups of samples were completely discriminated. To our knowledge, this is the first study using $^{1}$H-NMR based metabolomics to explore the characteristics of nutritional profiling of different kinds of freshwater fish soups and the state of *in vitro* digestion simulation. The metabolic changes in digested fish soups could reveal the information of chemical compounds which play important roles in the body. Furthermore, the metabolic patterns of different kinds of fish soups could also reflect the various nutritional profiling characteristics for dietary therapy.

**Acknowledgments:** Financial support was provided by the National Nature Science Foundation of China (No. 31772047 and 31501495), the Fundamental Research Funds for the Central Universities of China (No. 2662019PY031), and the China Agriculture Research System (CARS-45-27).

## References

1. S. Mol, Preparation and the shelf-life assessment of ready-to-eat fish soup, *European Food Research & Technology*, 2005**, 220**(3-4), 305-308.
2. B. N. Paul, S. Chanda, N. Sridhar and S. S. Giri In *Nutrient profile of some freshwater food fishes and its significance as health food*, XVI Biennial Animal Nutrition Conference, 2016.
3. M. B. Munir, R. Hashim, Y. H. Chai, T. L. Marsh and S. A. M. Nor, Dietary prebiotics and probiotics influence growth performance, nutrient digestibility and the expression of immune regulatory genes in snakehead (Channa striata) fingerlings, *Aquaculture*, 2016**, 460**, 59-68.
4. S. H. Baie and K. A. Sheikh, The wound healing properties of Channa striatus-cetrimide cream — tensile strength measurement, *Journal of Ethnopharmacology*, 2000**, 71**(1–2), 93-100.
5. J. Zhang, Y. Yao, X. Ye, Z. Fang, J. Chen, D. Wu, D. Liu and Y. Hu, Effect of cooking temperatures on protein hydrolysates and sensory quality in crucian carp ( Carassius auratus ) soup, *Journal of Food Science & Technology*, 2013**, 50**(3), 542-8.
6. V. Govindaraju, K. Young and A. A. Maudsley, Proton NMR chemical shifts and coupling constants for brain metabolites, *Nmr Biomed*, 2000**, 13**(3), 129-153.
7. G. Paglia, M. Stocchero, S. Cacciatore, S. Lai, P. Angel, M. T. Alam, M. Keller, M. Ralser and G. Astarita, Unbiased Metabolomic Investigation of Alzheimer's Disease Brain Points to Dysregulation of

Mitochondrial Aspartate Metabolism, *J Proteome Res*, 2016**, 15**(2), 608-618.

8. D. Tang, Y. Dong, H. Ren, L. Li and C. He, A review of phytochemistry, metabolite changes, and medicinal uses of the common food mung bean and its sprouts (Vigna radiata), *Chemistry Central Journal,8,1(2014-01-17)*, 2014**, 8**(1), 4.

9. A. Zakarova, J. Y. Seo, H. Y. Kim, J. H. Kim, J. H. Shin, K. M. Cho, C. H. Lee and J. S. Kim, Garlic sprouting is associated with increased antioxidant activity and concomitant changes in the metabolite profile, *Journal of Agricultural & Food Chemistry*, 2014**, 62**(8), 1875-80.

10. E. A. Petrakis, L. R. Cagliani, M. G. Polissiou and R. Consonni, Evaluation of saffron (Crocus sativus L.) adulteration with plant adulterants by (1)H NMR metabolite fingerprinting, *Food Chemistry*, 2015**, 173**, 890-896.

11. M. Palermo, G. Colla, G. Barbieri and V. Fogliano, Polyphenol metabolite profile of artichoke is modulated by agronomical practices and cooking method, *Journal of Agricultural & Food Chemistry*, 2013**, 61**(33), 7960-8.

12. A. D. Troise, R. Ferracane, M. Palermo and V. Fogliano, Targeted metabolite profile of food bioactive compounds by Orbitrap high resolution mass spectrometry: The “FancyTiles” approach, *Food Research International*, 2014**, 63, Part B**, 139-146.

13. A. Merchant, A. Richter, M. Popp and M. Adams, Targeted metabolite profiling provides a functional link among eucalypt taxonomy, physiology and evolution, *Phytochemistry*, 2006**, 67**(4), 402-8.

14. A. Kårlund, K. Hanhineva, M. Lehtonen, G. J. Mcdougall, D. Stewart and R. O. Karjalainen, Non-targeted metabolite profiling highlights the potential of strawberry leaves as a resource for specific bioactive compounds, *Journal of the Science of Food & Agriculture*, 2016.

15. V. Arbona, D. J. Iglesias and A. Gómez-Cadenas, Non-targeted metabolite profiling of citrus juices as a tool for variety discrimination and metabolite flow analysis, *BMC Plant Biology,15,1(2015-02-05)*, 2015**, 15**(1), 38.

16. Y. Jiang, J. Vaysse, V. Gilard, S. Balayssac, S. Déjean, M. Malet-Martino, B. David, C. Fiorini and Y. Barbin, Quality assessment of commercial Magnoliae officinalis Cortex by $^{1}$H-NMR-based metabolomics and HPLC methods, *Phytochemical Analysis*, 2012**, 23**(4), 387.

17. J. Wang, H.-L. Zeng, H. Du, Z. Liu, J. Cheng, T. Liu, T. Hu, G. M. Kamal, X. Li, H. Liu and F. Xu, Evaluation of metabolites extraction strategies for identifying different brain regions and their relationship with alcohol preference and gender difference using NMR metabolomics, *Talanta*, 2018**, 179**, 369-376.

18. B. K. Ko, H. J. Ahn, d. B. F. Van, C. H. Lee and Y. S. Hong, Metabolomic insight into soy sauce through (1)H NMR spectroscopy, *Journal of Agricultural & Food Chemistry*, 2009**, 57**(15), 6862.

19. N. J. Serkova and C. U. Niemann, Pattern recognition and biomarker validation using quantitative 1H-NMR-based metabolomics, *Expert Review of Molecular Diagnostics*, 2006**, 6**(5), 717.

20. C. Xiao, H. Dai, H. Liu, Y. Wang and H. Tang, Revealing the Metabonomic Variation of Rosemary Extracts Using 1H NMR Spectroscopy and Multivariate Data Analysis, *Journal of Agricultural & Food Chemistry*, 2008**, 56**(21), 10142.

21. Y. Liu, T. Chen, M.-H. Li, H.-D. Xu, A.-Q. Jia, J.-F. Zhang and J.-S. Wang, 1H NMR based metabolomics approach to study the toxic effects of dichlorvos on goldfish (Carassius auratus), *Chemosphere*, 2015**, 138**, 537-545.

22. X. Y. Tang, J. Chen, G. G. Li, L. J. Zhu and Y. F. Dai, Effect of processing conditions on th enutrition value of fish soup, *Science and Technology of Food Industry*, 2008**,** (10), 248-251.

23. Z. Lin, J. Y. Ren, G. W. Su, Y. Bao and M. M. Zhao, Comparison of in vitro digestion characteristics and antioxidant activity of hot- and cold-pressed peanut meals, *Food Chemistry*, 2013**, 141**(4), 4246.

24. F. E. Boland and D. D. Paige, Collaborative study of a method for the determination of trimethylamine nitrogen in fish, *Journal - Association of Official Analytical Chemists*, 1971**, 54**(3), 725-7.
25. M. Liu, X.-a. Mao, C. Ye, H. Huang, J. K. Nicholson and J. C. Lindon, Improved WATERGATE Pulse Sequences for Solvent Suppression in NMR Spectroscopy, *Journal of Magnetic Resonance*, 1998**, 132**(1), 125-129.
26. C. David, V. Palmira, C. M. M., S. M. Guillermo, H. Marta and H. Antonio, 1H‐HRMAS NMR study of smoked Atlantic salmon (Salmo salar), *Magnetic Resonance in Chemistry*, 2010**, 48**(9), 693-703.
27. A. Bordoni, L. Laghi, E. Babini, M. Di Nunzio, G. Picone, A. Ciampa, V. Valli, F. Danesi and F. Capozzi, The foodomics approach for the evaluation of protein bioaccessibility in processed meat upon in vitro digestion, *Electrophoresis*, 2014**, 35**(11), 1607-1614.
28. N. P. Vidal, G. Picone, E. Goicoechea, L. Laghi, M. J. Manzanos, F. Danesi, A. Bordoni, F. Capozzi and M. D. Guillen, Metabolite release and protein hydrolysis during the in vitro digestion of cooked sea bass fillets. A study by H-1 NMR, *Food Research International*, 2016**, 88**, 293-301.
29. Y. Wei, M. Liang, K. Mai, K. Zheng and H. Xu, 1H NMR‐based metabolomics studies on the effect of size‐fractionated fish protein hydrolysate, fish meal and plant protein in diet for juvenile turbot (Scophthalmus maximus L.), *Aquaculture Nutrition*, 2017**, 23**(3), 523-536.
30. Y. Liu, J. Cheng, H. Liu, Y. Deng, J. Wang and F. Xu, NMRSpec: An integrated software package for processing and analyzing one dimensional nuclear magnetic resonance spectra, *Chemometrics and Intelligent Laboratory Systems*, 2017**, 162**, 142-148.
31. Y. Liu, Y. Gao, J. Cheng, J. Wang and F. Xu, A Processing Method for Spectrum Alignment and Peak Extraction for NMR Spectra, *Chinese Journal of Magnetic Resonance*, 2015**, 2**, 382-392.
32. H. Du, J. Fu, S. Wang, H. Liu, Y. Zeng, J. Yang and S. Xiong, $^{1}$H-NMR metabolomics analysis of nutritional components from two kinds of freshwater fish brain extracts, *Rsc Advances*, 2018**, 8**, 19470-19478.
33. T. Liu, Z. He, X. Tian, G. M. Kamal, Z. Li, Z. Liu, H. Liu, F. Xu, J. Wang and H. Xiang, Specific patterns of spinal metabolites underlying α-Me-5-HT-evoked pruritus compared with histamine and capsaicin assessed by proton nuclear magnetic resonance spectroscopy, *Biochimica et Biophysica Acta (BBA) - Molecular Basis of Disease*, 2017**, 1863**(6), 1222-1230.
34. L. Zhang, L. Wang, Y. Hu, Z. Liu, Y. Tian, X. Wu, Y. Zhao, H. Tang, C. Chen and Y. Wang, Selective metabolic effects of gold nanorods on normal and cancer cells and their application in anticancer drug screening, *Biomaterials*, 2013**, 34**(29), 7117-7126.
35. Y. Jung, J. Lee, J. Kwon, K. Lee, D. H. Ryu and G. Hwang, Discrimination of the Geographical Origin of Beef by 1H NMR-Based Metabolomics, *Journal of Agricultural and Food Chemistry*, 2010**, 58**(19), 10458-10466.
36. S. Bhattacharyya, L. Pence, R. Beger, S. Chaudhuri, S. Mccullough, K. Yan, P. Simpson, L. Hennings, J. Hinson and L. James, Acylcarnitine profiles in acetaminophen toxicity in the mouse: comparison to toxicity, metabolism and hepatocyte regeneration, *Metabolites*, 2013**, 3**(3), 606-622.
37. C. Fagernes, S. Ellefsen, K. Stenslokken, M. Berenbrink and G. Nilsson, Molecular background to ethanol production in crucian carp ( Carassius carassius ), *Comparative Biochemistry & Physiology Part A Molecular & Integrative Physiology*, 2008**, 150**(3), S112.
38. C. H. Zhang, P. Z. Hong, S. G. Deng and Z. H. Jiang, Chemical characteristics of Perna viridis meat and its application to seafood seasoning, *Journal of Fisheries of China*, 2000, 267-270.
39. J. Zhang, Y. Yao, X. Ye, Z. Fang, J. Chen, D. Wu, D. Liu and Y. Hu, Effect of cooking temperatures on protein hydrolysates and sensory quality in crucian carp (Carassius auratus) soup, *Journal of Food Science and Technology*, 2013**, 50**(3), 542-548.

40. S. Murakami, The role of taurine in the pathogenesis of obesity, *Molecular Nutrition & Food Research*, 2015**, 59**(7), 1353-1363.
41. C. Madeddu, G. Mantovani, G. Gramignano and A. Macciò, Advances in pharmacologic strategies for cancer cachexia, *Expert Opinion on Pharmacotherapy*, 2015**, 16**(14), 2163-77.
42. L.-p. Sun, C.-j. Bao, J.-h. Liu, X.-j. Su and Y. Sun, Study on the preparation and antioxidation activities of polysaccharide secretion and mucopolysaccharide from Channa argus, *Food and Fermentation Industries*, 2015**, 41**(7), 81-85.
43. S. K. Sikder and A. Das, Isolation and characterization of glycosaminoglycans (mucopolysaccharides) from the skin of the fish Labeo rohita, *Carbohydrate Research*, 1979**, 71**(1), 273-285.
44. J. A. Cifonelli, Acid hydrolysis of acidic mucopolysaccharides, *Carbohydrate Research*, 1966**, 2**(2), 151-161.
45. M. B. Mathews, Animal mucopolysaccharidases. In *Methods in Enzymology*, Academic Press: 1966; Vol. 8, pp 654-662.

**Figure legends:**

**Fig.** 1. A series of 2D-NMR spectra for the identification of metabolite phenylalanine: (A): COSY; (B): HSQC; (C): HMBC.

**Fig.** 2 Representative 1H NMR spectra of fish soup samples. CCS: Crucian carp soup; SS: Snakehead soup; DCCS: Digested crucian carp soup; DSS: Digested snakehead soup. *Note: 1: fatty acids; 2: isoleucine; 3: leucine; 4: valine; 5: threonine; 6: lactate; 7: lysine; 8: alanine; 9: eicosapentaenoic fatty acid (ω-3; EPA C20:5); 10: acetic acid; 11: unsaturated fatty acids; 12: linoleic acid(ω-6; C18:2); 13: methionine; 14: docosahexaenoic fatty acid (DHA); 15: glutamate; 16: succinic acid; 17: glutamine; 18: aspartate; 19: asparagine; 20: creatine/Creatine phosphate; 21: phenylalanine; 22: choline; 23: phosporylcholine; 24: taurine; 25: glucose; 26: glycine; 27: Not identified; 28: ethanol.*

**Fig.** 3 Results of spectroscopic alignment with NMRSpec software.

**Fig.** 4. PCA derived from $^{1}$H-NMR spectra of all kinds of freshwater fish soup samples before and after *in vitro* gastro-intestinal digestion.

**Fig.** 5. PCA and OPLS-DA of the NMR spectrum for two kinds of fish soups. *Note: A: PCA; B: Scores plot for OPLS-DA; C: Loading plot for OPLS-DA, and the color bar corresponds to the weight of the corresponding variable in the discrimination of statistically significant (red) or not statistically significant (blue). Positive and negative peaks indicate a relative decrease and increase in the level of metabolite in the digested SS samples.*

**Fig.** 6. PCA and OPLS-DA of the NMR spectrum for two kinds of fish soups after *in vitro* simulated gastro-intestinal digestion. *Note: A: PCA; B: Scores plot for OPLS-DA; C: Loading plot for OPLS-DA, and the color bar corresponds to the weight of the corresponding variable in the discrimination of statistically significant (red) or not statistically significant (blue). Positive and negative peaks indicate a relative decrease or increase in the level of metabolite in the digested DSS samples.*

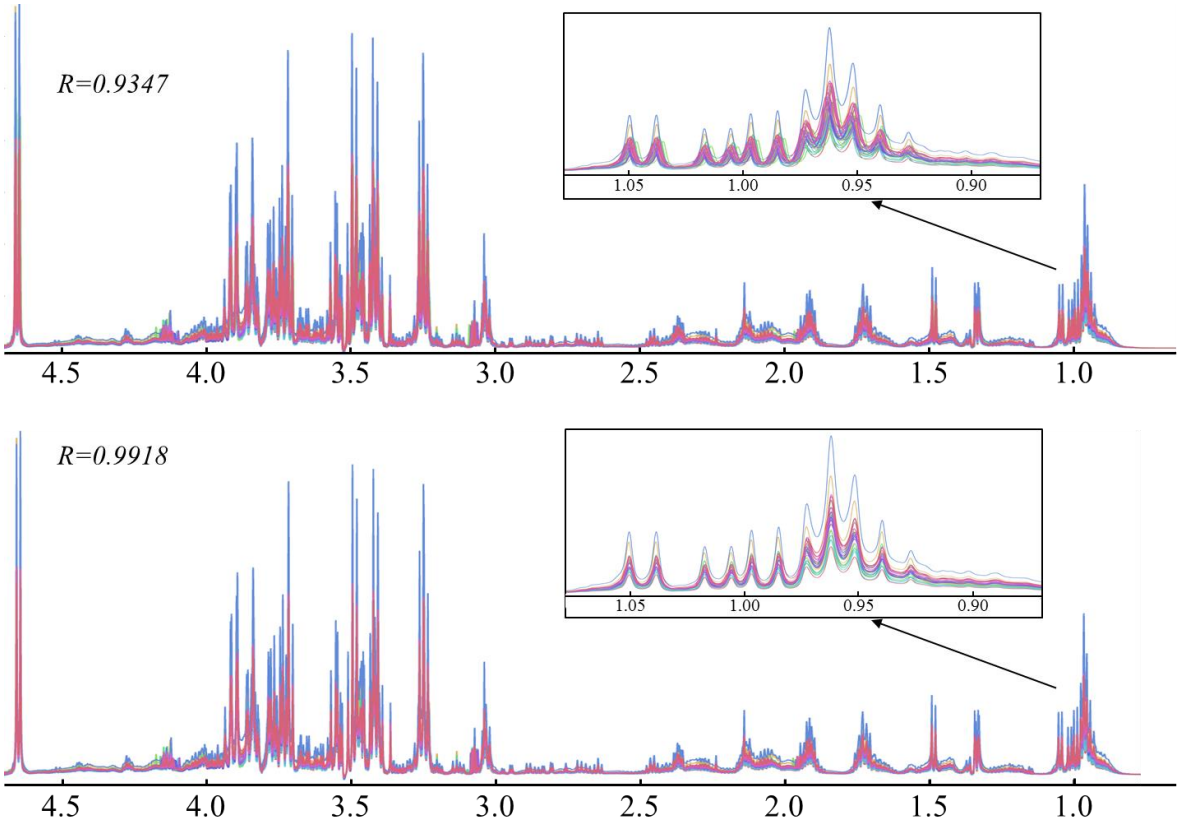


Fig. 1. Results of spectroscopic alignment with NMRSpec software.

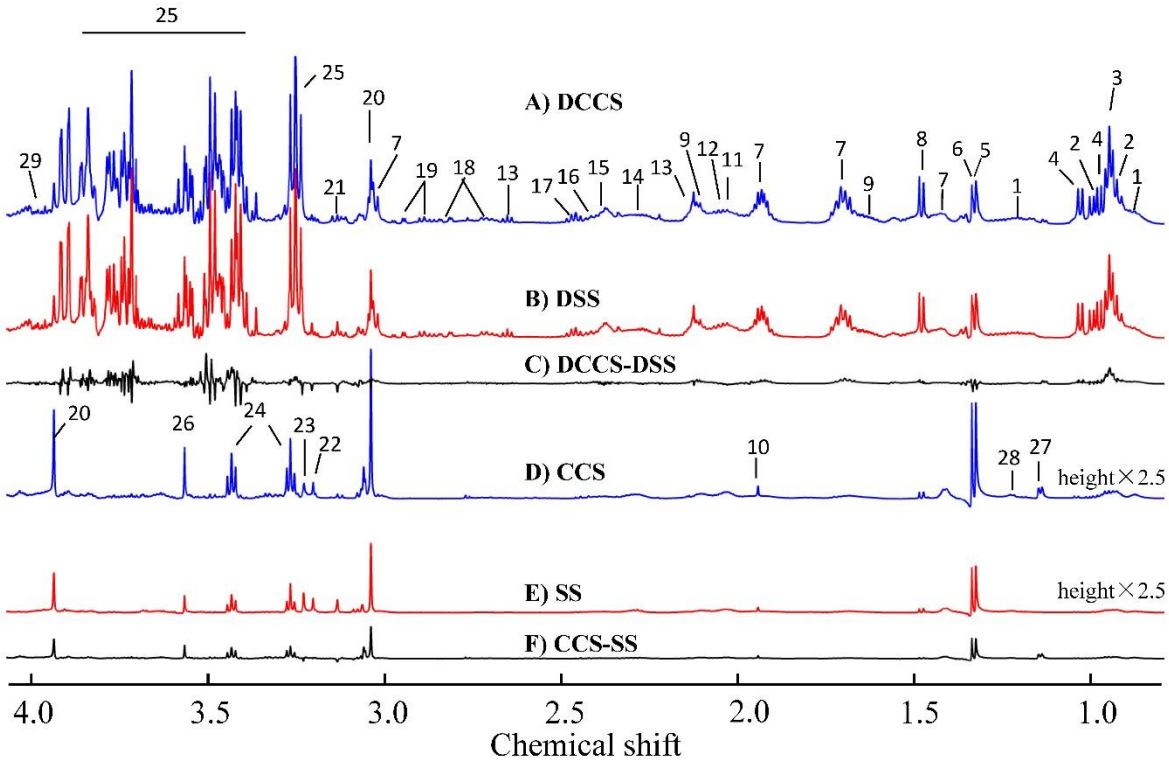


474

475 **Fig.** 2 Representative $^{1}$H NMR spectra of fish soup samples. CCS: Crucian carp soup; SS:
476 Snakehead soup; DCCS: Digested crucian carp soup; DSS: Digested snakehead soup; DSS-
477 DCCS: Differences between groups of DSS and DCCS; SS-CCS: Differences between groups
478 of SS and CCS. *Note: 1: fatty acids; 2: isoleucine; 3: leucine; 4: valine; 5: threonine; 6: lactate;*
479 *7: lysine; 8: alanine; 9: eicosapentaenoic fatty acid (ω-3; EPA C20:5); 10: acetic acid; 11:*
480 *unsaturated fatty acids; 12: linoleic acid(ω-6; C18:2); 13: methionine; 14: docosahexaenoic*
481 *fatty acid (DHA); 15: glutamate; 16: succinic acid; 17: glutamine; 18: aspartate; 19:*
482 *asparagine; 20: creatine/Creatine phosphate; 21: phenylalanine; 22: choline; 23:*
483 *phosporylcholine; 24: taurine; 25: glucose; 26: glycine; 27: Not identified; 28: ethanol.*

484

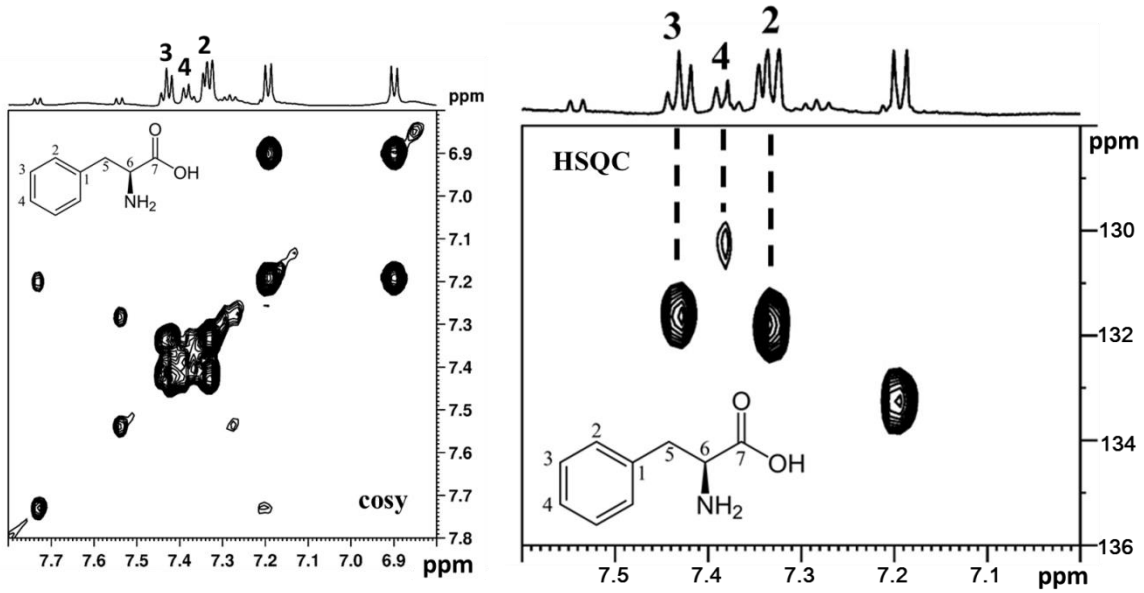


(A) COSY (B) HSQC

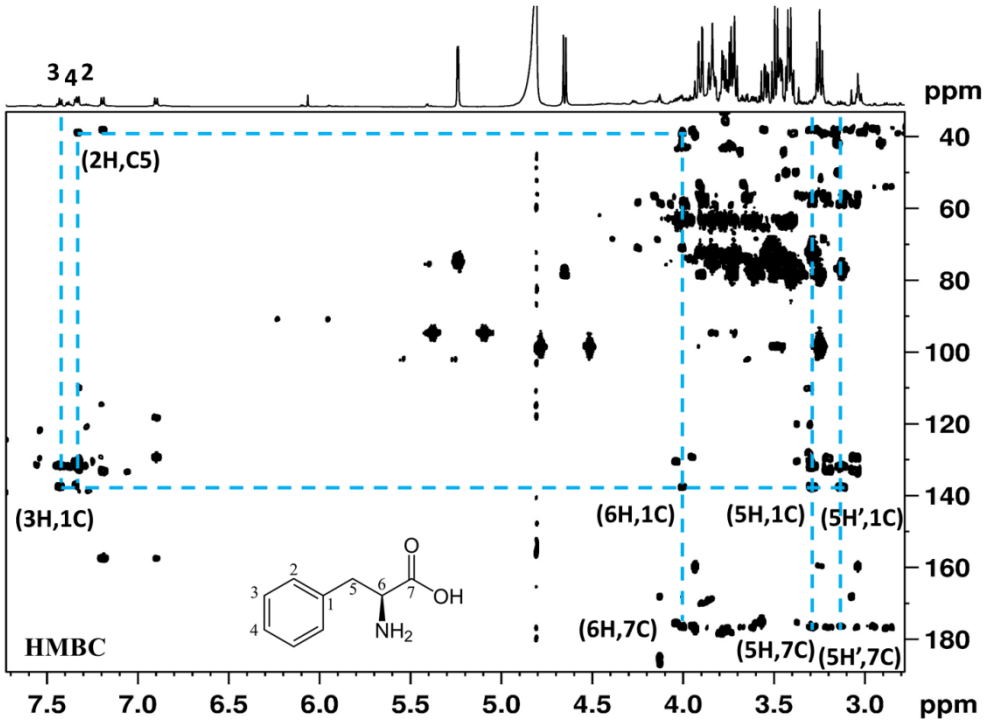


(C) HMBC

**Fig.** 3 A series of 2D-NMR spectra for the identification of metabolite phenylalanine: (A): COSY; (B): HSQC; (C): HMBC.

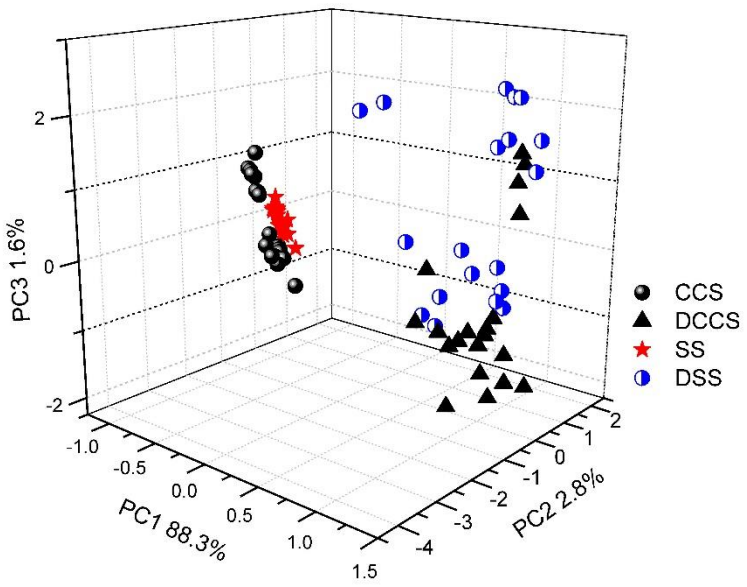


493

494 **Fig.** 4 PCA Analysis derived from $^{1}$H-NMR spectra of all kinds of freshwater fish soup samples

495 before and after *in vitro* gastro-intestinal digestion.

496

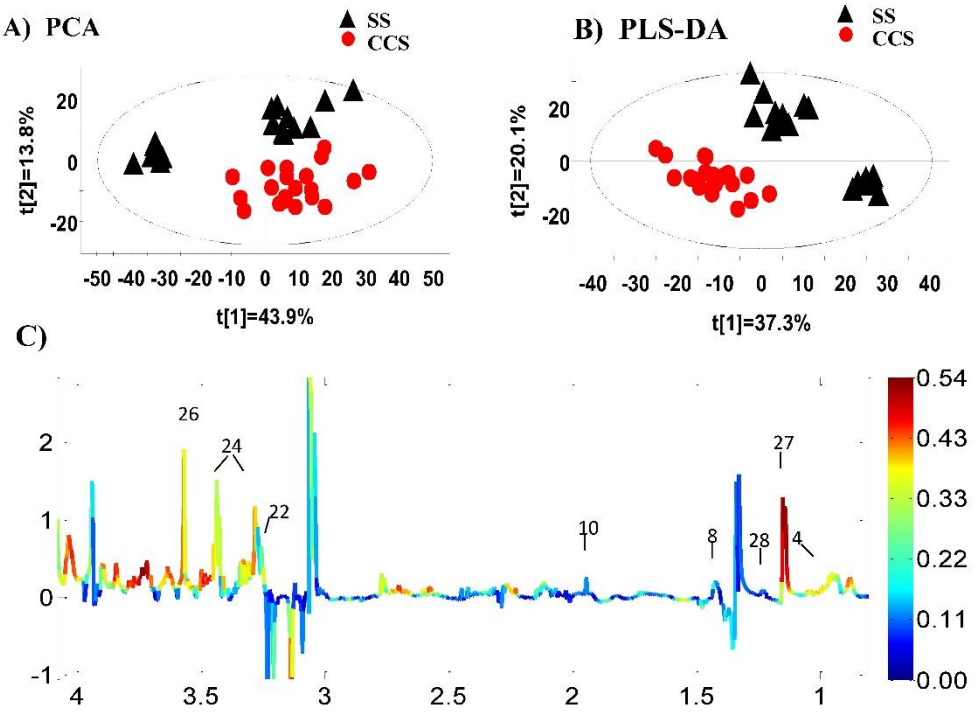


497

498

499 **Fig.** 5. PCA and OPLS-DA of the NMR spectrum for two kinds of fish soups. *Note: A: PCA;*

500 *B: Scores plot for OPLS-DA; C: Loading plot for OPLS-DA, and the color bar corresponds to*

501 *the weight of the corresponding variable in the discrimination of statistically significant (red)*

502 *or not statistically significant (blue). Positive and negative peaks indicate a relative decrease*

503 *and increase in the level of metabolite in the digested SS samples.*

504

505

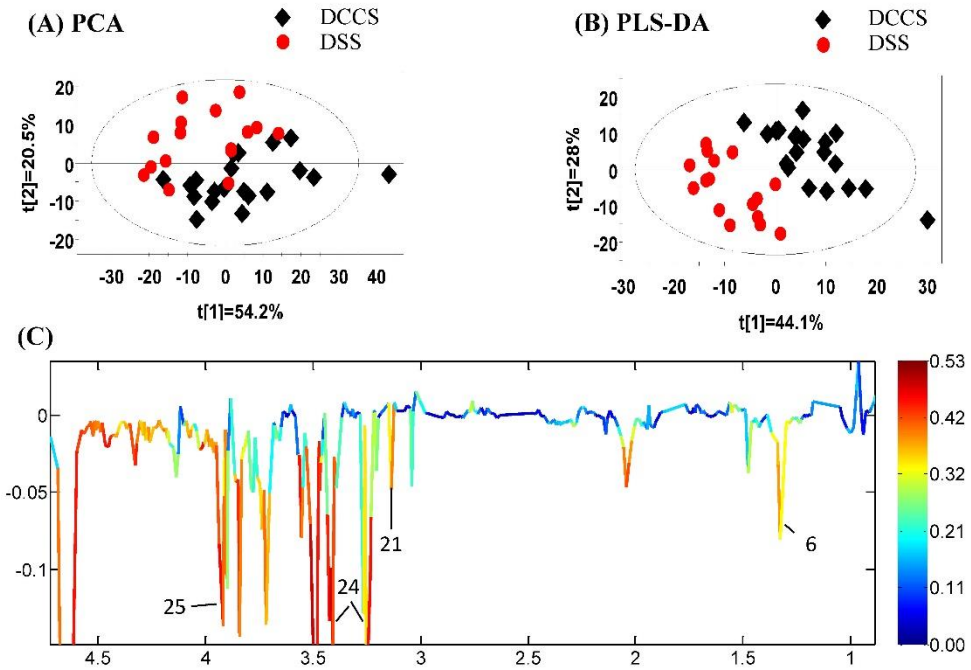


506

507 **Fig.** 6. PCA and OPLS-DA of the NMR spectrum for two kinds of fish soups after *in vitro*

508 simulated gastro-intestinal digestion. *Note: A: PCA; B: Scores plot for OPLS-DA; C: Loading*

509 *plot for OPLS-DA, and the color bar corresponds to the weight of the corresponding variable*

510 *in the discrimination of statistically significant (red) or not statistically significant (blue).*

511 *Positive and negative peaks indicate a relative decrease and increase in the level of metabolite*

512 *in the digested DSS samples.*